

## Numerical analysis of particle transport in low-pressure, low-temperature plasma environment

Heon Chang Kim\*

*Department of Chemical Engineering, Hoseo University, Asan, Chungnam 336-795, Korea*

(Received 7 October 2009, accepted 10 October 2009)

### Abstract

This paper presents simulation results of particle transport in low-pressure, low-temperature plasma environment. The size dependent transport of particles in the plasma is investigated with a two-dimensional simulation tool developed in-house for plasma chamber analysis and design. The plasma model consists of the first two and three moments of the Boltzmann equation for ion and electron fluids respectively, coupled to Poisson's equation for the self-consistent electric field. The particle transport model takes into account all important factors, such as gravitational, electrostatic, ion drag, neutral drag and Brownian forces, affecting the motion of particles in the plasma environment. The particle transport model coupled with both neutral fluid and plasma models is simulated through a Lagrangian approach tracking the individual trajectory of each particle by taking a force balance on the particle. The size dependant trap locations of particles ranging from a few nm to a few  $\mu\text{m}$  are identified in both electropositive and electronegative plasmas. The simulation results show that particles are trapped at locations where the forces acting on them balance. While fine particles tend to be trapped in the bulk, large particles accumulate near bottom sheath boundaries and around material interfaces, such as wafer and electrode edges where a sudden change in electric field occurs. Overall, small particles form a "dome" shape around the center of the plasma reactor and are also trapped in a "ring" near the radial sheath boundaries, while larger particles accumulate only in the "ring". These simulation results are qualitatively in good agreement with experimental observation.

**Key words :** Particle transport, Non-thermal plasma, Three-moment model, Electropositive plasma, Electronegative plasma

### 1. INTRODUCTION

Integrated circuits consist of multiple layers of patterned thin solid films. Patterning of very small features with large aspect ratios requires processes which preferentially etch in the vertical direction. Plasma etching and reactive ion etching have this capability

and are now the industry standard for VLSI and ULSI circuit production. In such plasma processes, particles are generated either through homogeneous or heterogeneous chemical reactions, and are typically tens of nm to tens of  $\mu\text{m}$  in diameter. The number density of the particles in low pressure, radio frequency plasmas is known to be as high as  $10^8 \text{ cm}^{-3}$  (Selwyn *et al.*, 1991).

The particles in the plasma become negatively charged by collecting electrons and ions, and as a result are levitated by the large electric field in the sheath region.

\*Corresponding author.

Tel : +82-(0)41-540-5752, E-mail : heonchan@Hoseo.edu

The levitated particles are subject to various forces acting on them and can become confined in regions where those forces balance. The extinction of the plasma at the end of a wafer processing step thus leads to particles depositing on the wafer surface, resulting in a circuit defect. To reduce defect density and to improve circuit performance, reliability and yield, particle dynamics in a plasma reactor need to be well understood for contamination control. This can be facilitated by a comprehensive plasma reactor model. Such a model will also aid in pollution prevention through identification of operating conditions which minimize the formation of undesirable byproducts, while maintaining or even increasing chip yield, and through elimination of the extensive experimentation currently used in equipment and process design (Kim and Manousiouthakis, 2000).

In this paper, the transport of particles in capacitively coupled, parallel plate, rf plasma reactors with a single wafer is simulated by VIP-SEPCAD (Virtual Integrated Prototyping Simulation Environment for Plasma Chamber Analysis and Design) developed in-house, and the effects of the particle size on the particle motion and consequently on the steady-state distribution of particles in the plasma reactors are investigated. A two dimensional three moment model is employed to predict plasma properties which have major effects on particle behavior in the plasma reactor. Individual particle trajectories are tracked, using a Lagrangian approach that takes into account the various forces acting on the particle. Gravitational, electrostatic, ion drag, neutral drag and Brownian forces are considered to describe the particle motion in the plasma environment. Two case studies are performed. The first case deals with an electropositive plasma. In this case, transport models for the plasma and the particle are decoupled by assuming that the plasma is not affected by the presence of particles. Neutral flow fields are evaluated using an analytical solution that is based on axisymmetric stagnation point flow with a low Reynolds number. Furthermore, the thermophoretic effect is not manifested, since an isothermal assumption is employed in the neutral model.

In the second case study, the particle model is simulated, without the aforementioned simplifying assumptions, for an electronegative plasma by coupling the plasma and neutral fluid models

## 2. MODEL DESCRIPTION

The plasma model employed in this study consists of continuity, momentum and energy equations, for each charged species, derived from the first three moments of the Boltzmann equation. Since this three moment model has been previously described in detail (Kim and Manousiouthakis, 1998), only a brief description is provided. Governing equations in this three moment model are analogous to the Euler equations of gas dynamics except additional terms quantifying elastic and inelastic collisions, electric field forces and thermal conductivity. The electric field is self-consistently determined from Poisson's equation with boundary conditions specified in a manner that Gauss's law is satisfied for all discontinuous surfaces between different materials. Use of such boundary conditions at the surfaces of powered and grounded electrodes enables evaluation of self-dc biases, in turn determination of ion bombardment energies. The plasma model utilized in this study has been implemented with a simplified version of the implicit ENO scheme in the VIP-SEPCAD (Kim and Sul, 2003). The efficient numerical algorithm developed for the rapid evaluation of time-periodic steady state solution (Kim *et al.*, 2004) is also utilized. For the particle transport model, using a Lagrangian approach, individual particle trajectory is tracked by solving Newton's equation of motion with the consideration of gravitational, electrostatic, ion drag, neutral drag, Brownian forces acting on the particle. The detailed models employed for these forces can be also found elsewhere (Kim and Manousiouthakis, 2001). In the calculation of these forces, particles are assumed to be spheres, and information flows among the plasma, neutral and particle transport models are illustrated in Figure 1.

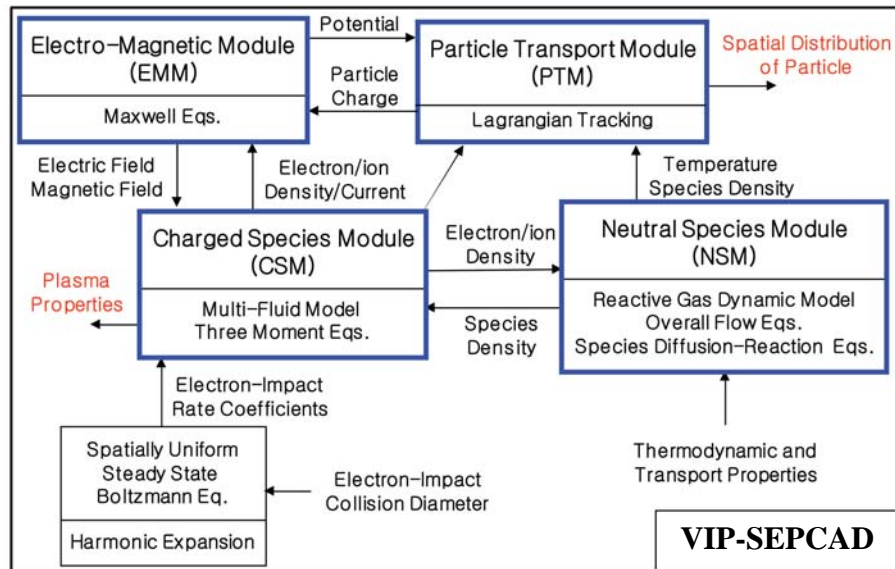


Figure 1. Information flows among plasma, neutral and particle transport models in VIP-SEPCAD.

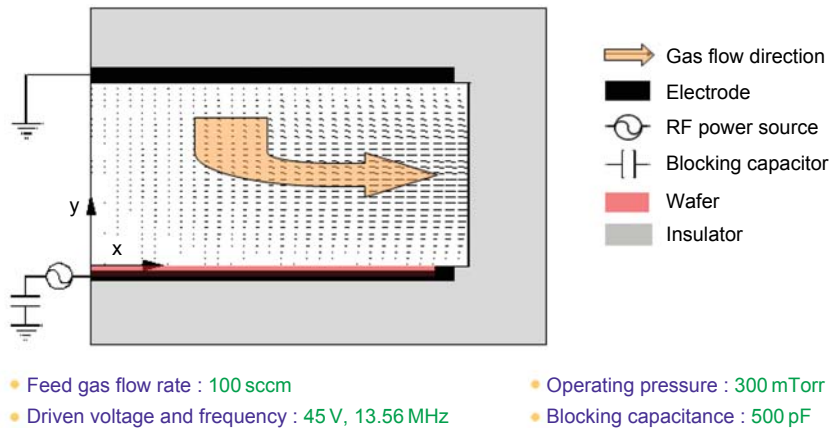


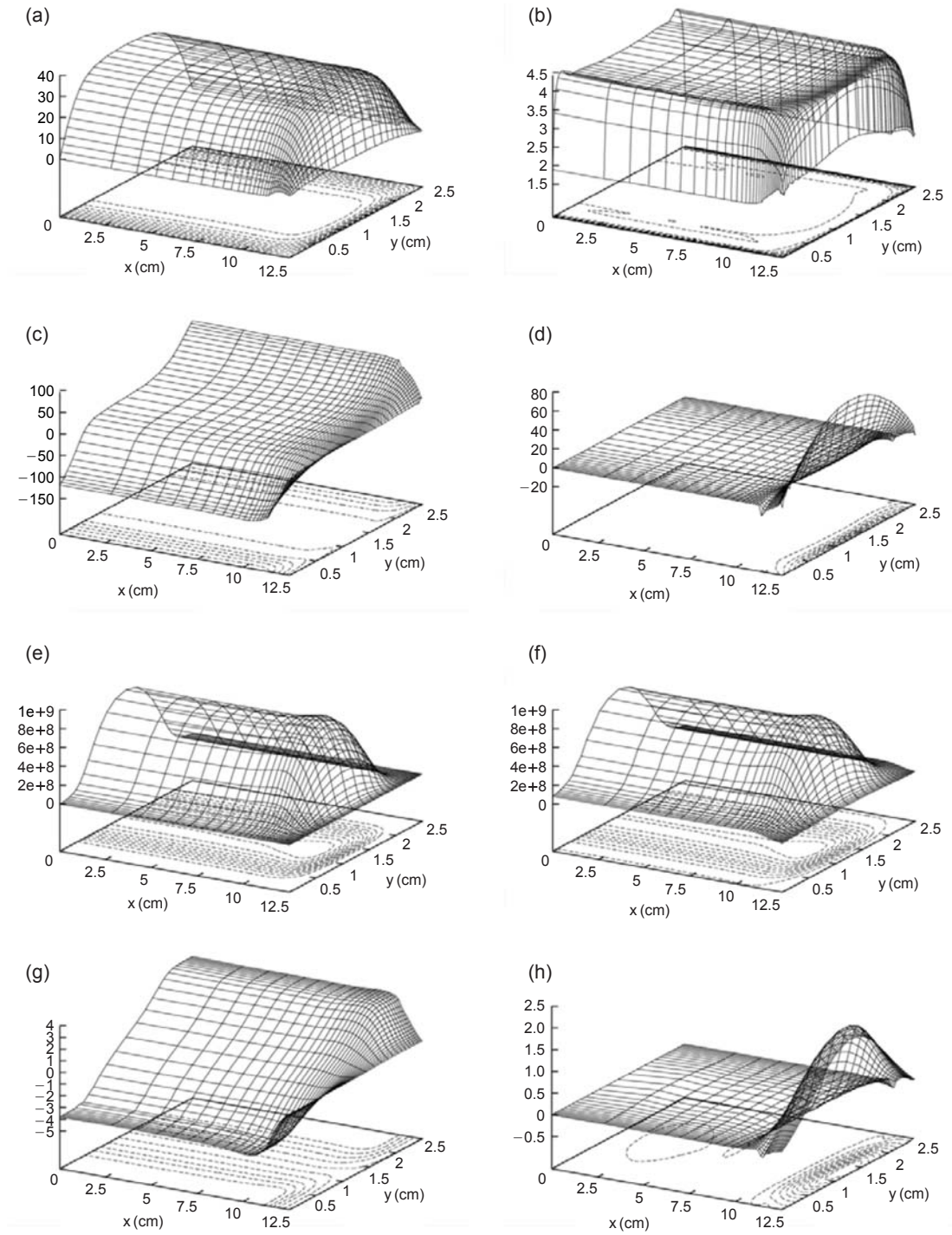
Figure 2. Schematic configuration of plasma reactor considered for electropositive plasma case.

### 3. RESULTS AND DISCUSSION

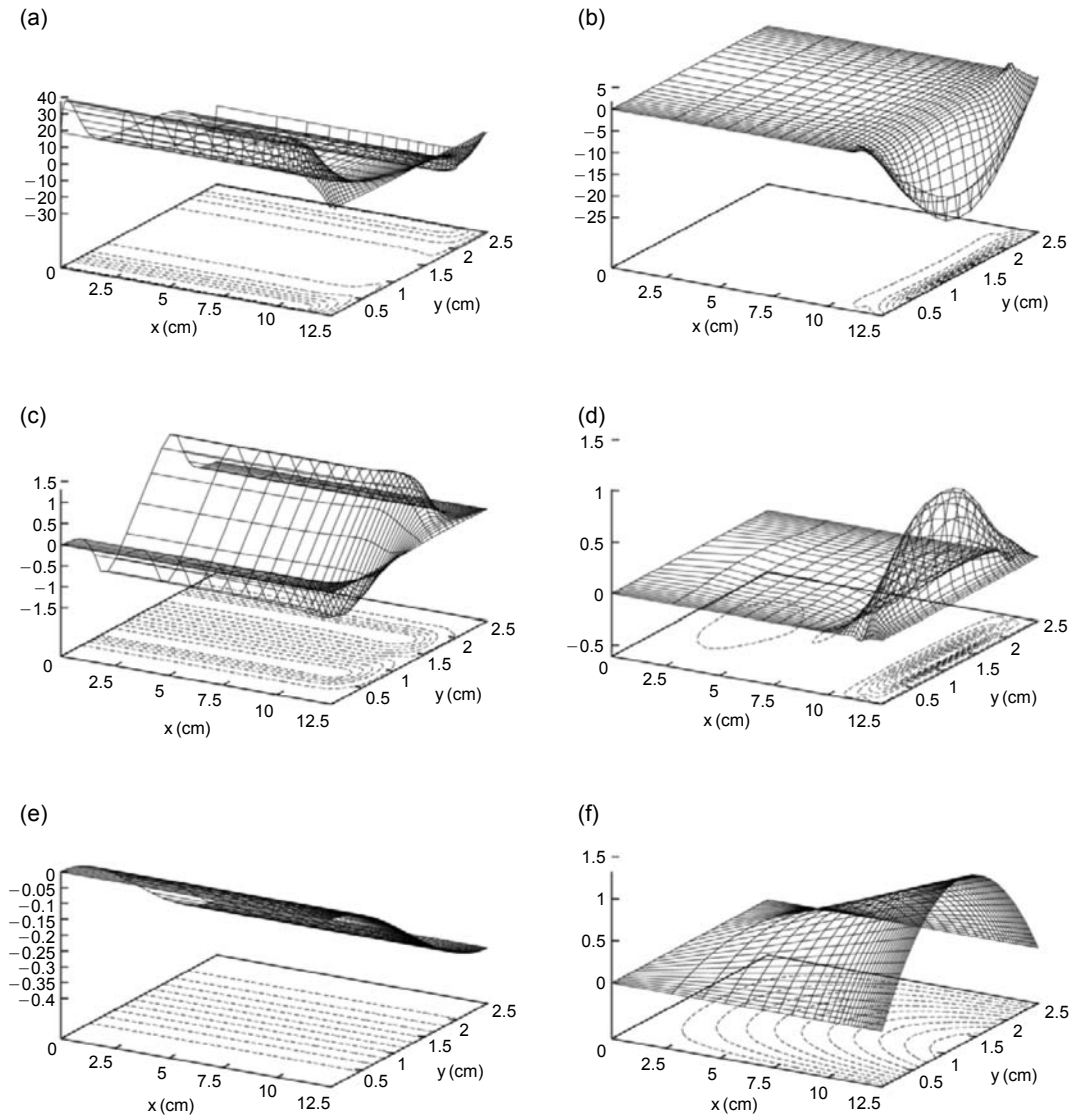
#### 3.1 Electropositive plasma case

Figure 2 shows the schematic configuration of the plasma reactor, considered for the electropositive plasma case, with uniform inflow of pure argon through a shower head and radial outflow. Assuming axisym-

metric flow, only half of the reactor becomes a computational domain. In this simulation, the advective flow field of argon gas entering the plasma reactor at uniform velocity was obtained from an approximate analytical solution by assuming axisymmetric stagnation point flow with the wall Reynolds number less than 1 as described in (Kim and Manousiouthakis, 2001). Other simulation parameters and conditions can be also



**Figure 3.** Time-averaged plasma properties: (a) electric potential (V), (b) electron temperature (eV), (c) axial electric field ( $\text{Vcm}^{-1}$ ), (d) radial electric field ( $\text{Vcm}^{-1}$ ), (e) electron density ( $\times 10^9 \text{ cm}^{-3}$ ), (f) ion density ( $\times 10^9 \text{ cm}^{-3}$ ), (g) axial ion flux ( $\times 10^{13} \text{ cm}^{-2} \text{ sec}^{-1}$ ), (h) radial ion flux ( $\times 10^{13} \text{ cm}^{-2} \text{ sec}^{-1}$ ).



**Figure 4.** Various forces ( $\times 10^8$  dyne) acting on stationary particle of 1  $\mu\text{m}$  size: (a) axial electrostatic force, (b) radial electrostatic force, (c) axial ion drag force, (d) radial ion drag force, (e) axial neutral drag force, (f) radial neutral drag force.

found thereafter.

The time-averaged plasma properties affecting particle motion and corresponding forces acting on the particle of 1  $\mu\text{m}$  size are shown in Figure 3 and Figure 4 respectively. Since the electron temperature is much higher than the ion temperature, the charge accumulated on the particle is approximately proportional to the electron temperature. Furthermore the electron

charge number of the particle is linearly proportional to the particle size. The electrostatic force exhibits maxima around the sheath boundary due to a large electric field in the sheath region where the electric potentials drop sharply. Thus the electrostatic force pushes the negatively charged particles towards the bulk region. Since the particle charge is linearly dependent on the size, the electrostatic force would be also

proportional to the particle size. Meanwhile the ion drag force heavily depends on the ion velocity and density. Since the ions become supersonic when they enter the sheath region while the ion density decreases, the ion drag force has the largest value near the sheath boundary like the electrostatic force. However the ion drag force pushes the particles in the ion flow direction, toward the wall. As a consequence, these two forces balance around the sheath boundaries. The axial neutral drag force is an increasing function of the distance from the bottom electrode since neutral gas flows from the top electrode to the bottom electrode. Similarly, the radial neutral drag force is also an increasing function of the distance from the centerline. The ion drag and neutral drag forces are proportional to the particle cross-sectional area. Therefore, as the particle size increases, the ion drag and neutral drag forces increase much faster than the electrostatic force. Thus larger particles would be pushed more toward the bottom and side walls. The gravitational force is proportional to the particle volume and the Brownian force is proportional to the square root of the size. Hence, it is necessary to include the gravitational force as the particle size increases and the Brownian force as the particle size decreases.

With the aforementioned information on how various forces act on the particle, the effect of the particle size on the trapped location of particle was investigated by dividing the particle size into three groups;  $d_p = 1 \sim 10 \mu\text{m}$ ;  $d_p = 0.1 \sim 1 \mu\text{m}$ ; and  $d_p = 0.01 \sim 0.1 \mu\text{m}$ . In each simulation,  $10^4$  particles were used with the random initial position. Although not shown here, it was observed that the particles far away from the sidewall are trapped around the axial sheath boundaries, and then follow a contour on which axial forces acting on them balance. The final trapped locations of particles are shown in Figure 5. Particles larger than about 50 nm in diameter are confined near the radial sheath boundary. As discussed earlier, as the particle size increases, the ion drag and neutral drag forces increase much faster than the electrostatic force such that larger particles are pushed toward the sidewall, resulting in a

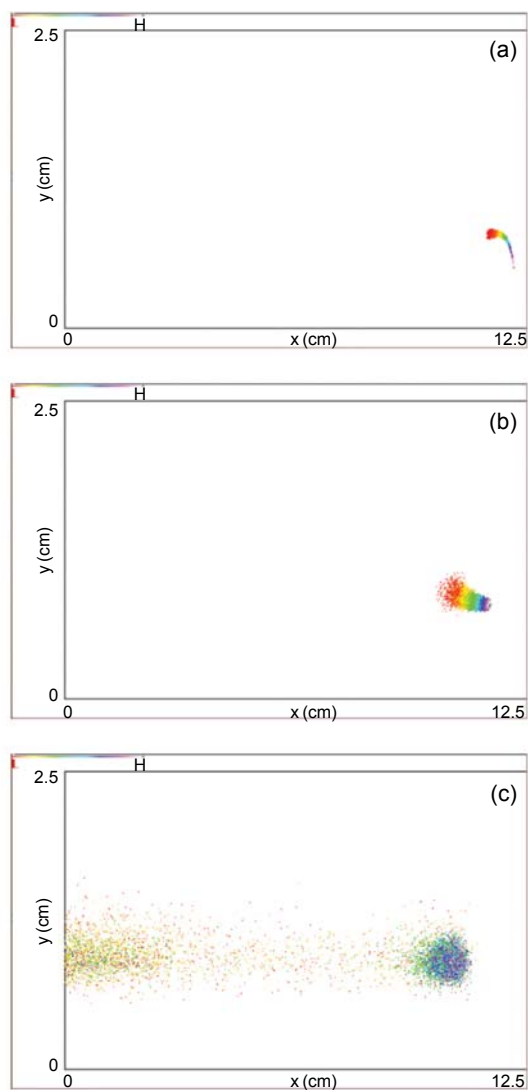


**Figure 5.** Size dependant trapped location of particles in electropositive plasma: (a)  $d_p = 1 \sim 10 \mu\text{m}$ , (b)  $d_p = 0.1 \sim 1 \mu\text{m}$ , (c)  $d_p = 0.01 \sim 0.1 \mu\text{m}$ .

wider “ring”. Meanwhile, particles smaller than about 50 nm in diameter accumulate both in a “dome” and in a “ring” depending on their initial location. Superposition of Figures 5(a), 5(b) and 5(c) reproduces the dome shape of particle clouds around the center and the ring shape near the radial sheath boundary, in qualitative agreement with experimental observation (Selwyn *et al.*, 1991).



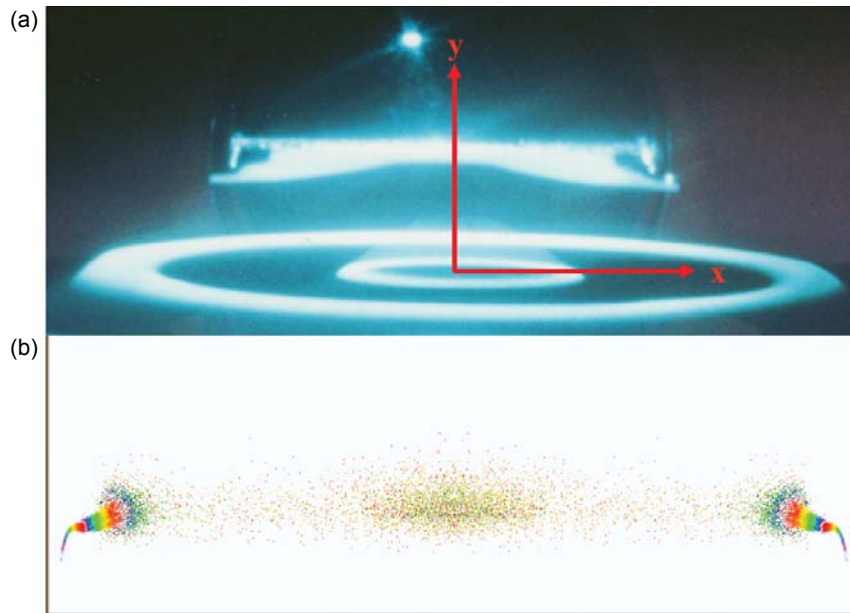


**Figure 6.** Structured particle cloud in argon plasma: (a) experimental observation by Selwyn *et al.* (1991), (b) simulation result by this work.

### 3.2 Electronegative plasma case

In this section, an oxygen plasma process, extensively utilized in etching photoresists as well as in depositing oxide films, is simulated with a three moment plasma model coupled with detail chemistry and transport of neutrals including metastables. Particle behavior in the oxygen plasma is simulated also for a capacitively coupled rf plasma processing tool. Applied voltage and frequency at the bottom electrode of 8 cm in radius were 150 V and 13.56 MHz respectively. Top and side walls of the reactor chamber were grounded. The height and radius of the reactor were 2 cm and 10 cm respectively. Pure oxygen gas was considered to be injected into the reactor at 100 sccm, 500 mTorr and 323 K through pin holes in the top electrode, and flows out through the rim around the bottom electrode and finally to a pumping port.

At the typical operating conditions of oxygen plasma, electron density is about two orders of magnitude lower than ion densities. Particle charges in such electronegative plasma are much lower than those in electropo-

sitive plasma. Consequently, the effect of the electrostatic field on particle transport decreases. Furthermore, due to the low number of simulated particles in addition to the low particle charging, the presence of the charged particle hardly affects the plasma itself. Only a small perturbation in the positive ion velocity, near the location where large particles are trapped, is observed during simulations. Figure 7 show trapped locations of particles in the oxygen plasma. Due to the low particle charging, particles larger than 1  $\mu\text{m}$  flow out to the pumping port. Figure 7(a) clearly shows that large particles are trapped near the electrode edge where a sudden change of electric field occurs. Therefore it is expected that particles larger than a critical size, depending on operating conditions, are trapped near the material interface such as wafer edges. The overall structure of the trapped dust cloud is similar to that in the electropositive case. Very fine dusts are trapped and scattered in the bulk, as shown in Figure 7(c), since their motion is hardly influenced by the neutral flow.

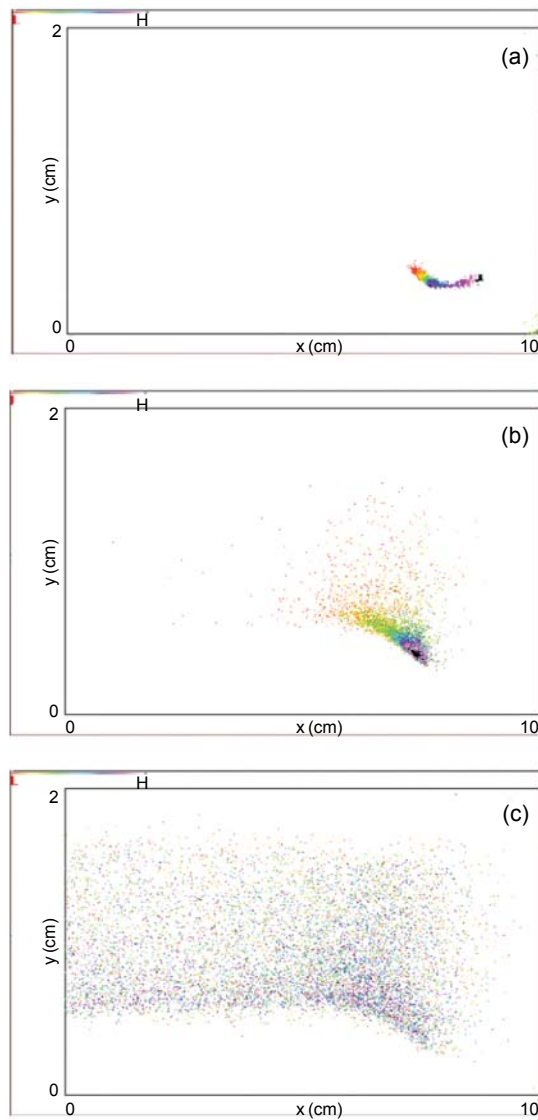


**Figure 7.** Size dependant trapped location of particles in electronegative plasma: (a)  $d_p = 0.1 \sim 1 \mu\text{m}$ , (b)  $d_p = 0.01 \sim 0.1 \mu\text{m}$ , (c)  $d_p = 0.001 \sim 0.01 \mu\text{m}$ .

#### 4. CONCLUSIONS

Two dimensional rf simulation results, for different particle sizes, with plasma, neutral and particle transport models were presented. The transport of particles

in the parallel plate plasma reactor was investigated to identify the effects of the particle size on the trapped location. Through a Lagrangian approach, individual particle trajectories were tracked by taking into account gravitational, electrostatic, ion drag, neutral drag, and Brownian forces. The simulation results are qualitatively in good agreement with experimental observation. Particles are trapped around the axial sheath boundary near the bottom electrode at the plasma condition considered in this study. They follow contours which eventually lead them to “trap” locations in the plasma. Fine particles tend to accumulate both in a “dome” around the center of the reactor and in a “ring” near the radial sheath boundaries, while larger particles accumulate only in the “ring”. Behavior of particles in other plasma sources may differ from that in the capacitively coupled plasmas. For example, in low pressure, high density plasmas such as inductively coupled plasmas, plasma density is usually about two orders of magnitude higher than the capacitively coupled plasmas. Hence ion drag forces, which are directly affected by the plasma density, may become a dominant factor affecting transport of particles. As a result, particles of moderate sizes may be swept out of the plasma in such systems.

#### REFERENCES

- Kim, H.C., and Manousiouthakis, V.I. (1998). Dually driven radio frequency plasma simulation with a three moment model, *Journal of Vacuum Science & Technology. A*, 16, 2162-2172.
- Kim, H.C., and Manousiouthakis, V.I. (2001). Dust transport phenomena in a capacitively coupled plasma reactor, *Journal of Applied Physics*, 89, 34-41.
- Kim, H.C., and Manousiouthakis, V.I. (2000). Simulation based plasma reactor design for improved ion bombardment uniformity, *Journal of Vacuum Science & Technology. B*, 18, 841-847.
- Kim, H.C., and Sul, Y.T. (2003). Development of virtual integrated prototyping simulation environment of plasma chamber analysis and design (VIP-SEPCAD), *Journal of the Korean Society of Semiconductor Equipment Technology*, 2, 9-12.



- Kim, H.C., Sul, Y.T., and Manousiouthakis, V.I. (2004) On rapid computation of time periodic steady state in simulation of capacitively coupled RF plasma, *IEEE Transactions on Plasma Science*, 32, 399-404.
- Selwyn, G.S., Heidenreich, J.E., and Haller, K.L. (1991). Rastered laser light scattering studies during plasma processing: Particle contamination trapping phenomena, *Journal of Vacuum Science & Technology. A*, 9, 2817-2824.